Article

JFPE

Journal of Fire Protection Engineering
23(2) 135–151

DOI: 10.1177/1042391512474666
jfe.sagepub.com

SAGE

Structural damage evaluation of reinforced concrete beams exposed to high temperatures

Eun Gyu Choi
CS Structural Engineering Inc., South Korea

Yeong-Soo Shin and Hee Sun Kim
Department of Architectural Engineering, Ewha Womans University, South Korea

Abstract
The objective of this study is to investigate the effect of temperature distribution, concrete strength, cover thickness, and heating time on the structural behavior of reinforced concrete beams. Toward this goal, reinforced concrete beams with different concrete compressive strength and cover thickness are fabricated and subjected to furnace heating for 60, 90, and 120 min under a loaded state. In order to analyze structural behavior based on the thermal behavior of the beams, transient temperature distribution is measured during the furnace heating. After furnace heating, spalling is observed. From loading tests performed on the damaged reinforced concrete beams, residual strength, maximum loads, and beam deflections are measured and examined. The experimental results show that significant damage occurs in the reinforced concrete beams under high temperatures. In addition, it is found that thermal and structural behavior of damaged reinforced concrete beams is dependent on cover thickness and concrete strength and that most structural damage occurs in a relatively short period of heating time. Using these experimental findings, an equation is proposed that can be used to predict maximum load capacity and stiffness reduction ratio of the damaged reinforced concrete beams.

Keywords
Reinforced concrete beams, normal-strength concrete, high-strength concrete, concrete load reduction, concrete stiffness reduction, structures in fire

Corresponding author:
Hee Sun Kim, Department of Architectural Engineering, Ewha Womans University, South Korea.
Email: hskim3@ewha.ac.kr

Introduction

Experimental studies to define changes of material properties and spalling of concrete due to fire have been reported for many years. Among them, the effect of high temperatures on material properties of normal concrete was examined by Harmathy [1,2]. Harmathy [1,2] reported experimental results for the temperature-dependent thermo-mechanical material properties, such as effective specific heat (thermal capacity), thermal conductivity, mass change rate, and thermal expansion of normal and lightweight concrete having different types of aggregate and mixture ratios. These material properties can also be found from ACI Committee 216 [3] and ENV [4]. For high-strength concrete (HSC) materials, temperature-dependent thermal, and mechanical material properties were reported by Kodur and Sultan [5] and Cheng et al. [6]. The former performed experiments for thermal material properties of HSC at different temperature levels, and the latter examined stress–strain curves of HSC at different temperature levels. Furthermore, Kodur et al. [7], Kodur and McGrath [8], and Kodur and Phan [9] reported experimental results for thermal and structural behavior of HSC columns. In their studies, the fire resistance of HSC columns was lower than that of normal-strength concrete (NSC) columns due to spalling. Spalling occurs when the tensile strength of concrete decreases and pore pressure increases as temperature increases [10]. An increase of pore pressure in HSC at elevated temperatures was reported by Kalifa et al. [11]. In their study, pore pressure was measured at different locations of NSC and HSC specimens at temperatures of 600°C. For HSC, peak pore pressure was measured as 3.7 MPa at 600°C and the location was 50 mm away from the surface. Kodur and Phan [9] examined the factors that could affect fire resistance of HSC columns [9], and these were fire intensity, fire size, heat output, heating rate, concrete strength, fiber reinforcement, types of aggregates, tie spacing, tie configuration, load levels, size of the member, etc. Especially, it was found that tie configurations affected the fire endurance of HSC columns by confining longitudinal rebar and concrete, thus minimizing the extent of spalling.

Relatively few studies have been reported about the fire endurance of reinforced concrete (RC) beams. Lee [12], Shin [13], Kim [14], and Choi [15] performed experimental studies for thermal and structural behavior of RC beams at elevated temperatures having different concrete strength. Lee [12] performed heating tests on NSC beams at elevated temperatures, while Shin [13] performed on these HSC beams. According to their studies, HSC beams showed higher temperatures and more damage due to spalling compared to NSC beams. In addition, it was found that the spalling occurred on the upper part of beam side surfaces for HSC beams due to high pore pressure developed in the upper part of the beam during heating. Using experimental results from Lee [12] and Shin [13], Kim [14] proposed non-destructive test methods evaluating the strength of fire damaged RC beams and found that the degraded strength of fire-damaged concrete could be recovered to some degree as time passes after a fire. Choi [15] reported the effect of many

parameters including concrete strength and cumulative temperatures on structural performance of RC beams using the existing experimental findings. In addition, Haj-Ali et al. [16] and Choi et al. [17] proposed a modeling technique for predicting temperature distributions and deformations of structural members. The proposed modeling technique, including temperature-dependent thermo-mechanical material properties of concrete during transient heating, was validated by comparing the prediction with the experimental results on RC beams.

This article aims to investigate the structural capacity of RC beams when exposed to high temperatures. Structural capacities of RC beams damaged by high temperatures are quantified by measuring load–deflection relationships and crack propagation from the four-point loading tests. The effects of concrete strength, cover thickness, and time period of heating on the thermal and structural behavior of damaged RC beams are also investigated. The experimental results are expected to help predict structural capacity of fire damaged RC beams and to find parameters that can prevent possible damage of RC beams under high temperatures.

Experimental program

Test specimens and parameters

Experiments consist of furnace heating and four-point loading tests on RC beams. For the tests, twelve RC beams are fabricated using ordinary Portland cement and pulverized fly ash. The fine and coarse aggregates are medium zone quartz sand and siliceous gravel, respectively, which are popularly used in Korea. The mix proportions for NSC and HSC are listed in Table 1. The steel reinforcements are D22 (deformed bars with diameter of 22 mm) and D10 bars (deformed bars with diameter of 10 mm). Measured tensile strength from the tests are 439 and 390 MPa for D22 and D10 bars, respectively. Test parameters are compressive strength of concrete, cover thickness, and time period of heating, as listed in Table 2. Sizes of the RC beams are 250 mm in width, 400 mm in depth, and 4700 mm in length, as illustrated in Figure 1(a). Details of the tested beam section with locations of

Table 1. Mix proportions of concrete.

Concrete types	W/C (%)	S/A (%)	C (kg/m^3)	S (kg/m^3)	G (kg/m^3)	Ad (%)
NSC	51.2	49.8	315	893	913	1.71
HSC	31	41	542	666	974	1.6

NSC: normal-strength concrete; HSC: high-strength concrete.

Table 2. List of tested beams.

Specimen	Time period of furnace test (min)	Applied load (kN)	Strength of concrete (MPa)	Cover thickness (mm)
N[a]4[c]-0[e]	0	–	21	40
N4-1[f]	60	87.1	21	40
N4-2[g]	120	87.1	21	40
N5[d]-0	0	–	21	50
N5-1	60	87.1	21	50
N5-2	120	87.1	21	50
H[b]4-0	0	–	55	40
H4-1	60	96.3	55	40
H4-2	90	96.3	55	40
H5-0	0	–	55	50
H5-1	60	96.3	55	50
H5-2	90	96.3	55	50

[a]N: normal strength concrete; [b]H: high strength concrete; [c]4: cover thickness = 40 mm; [d]5: cover thickness = 50 mm; [e]0: no furnace test; [f]1: 60 min furnace test; [g]2: 90 or 120 min furnace test.

thermocouples are illustrated in Figure 1(b). Three thermocouples are placed in the middle of beam length to measure the temperature distributions inside the beam during the furnace heating, as shown in Figure 1(b). These three measured points are located at 50, 200, and 350 mm from the bottom of a beam, and designated as 'Low', 'Mid', and 'Up', respectively. In order to investigate the effect of cover thickness on the behavior of the RC beams, cross-sectional areas are maintained as 250×400 mm, and cover thicknesses of the beams are varied between 40 and 50 mm.

Furnace heating

For furnace heating, RC beams are cured for over 6 months to prevent effect of excessive moisture and then placed in a heating furnace, as illustrated in Figure 2. The two side surfaces and bottom surface of the RC beams are under the effect of flame provided by the heating furnace. Prior to heating, the RC beams are subjected to loads in order to simulate the fire situation that occurs while the beam is being used as a structural member. The magnitude of the applied load is calculated from combined dead load and 40% of live load for an office building, as listed in Table 2. The applied load is maintained throughout the heating for 60, 90, or 120 min. Because the HSC beams failed due to excessive deflection earlier than 120 min of furnace heating, furnace heating of HSC beams is terminated at 90 min. The temperature of the heating furnace is controlled to follow the

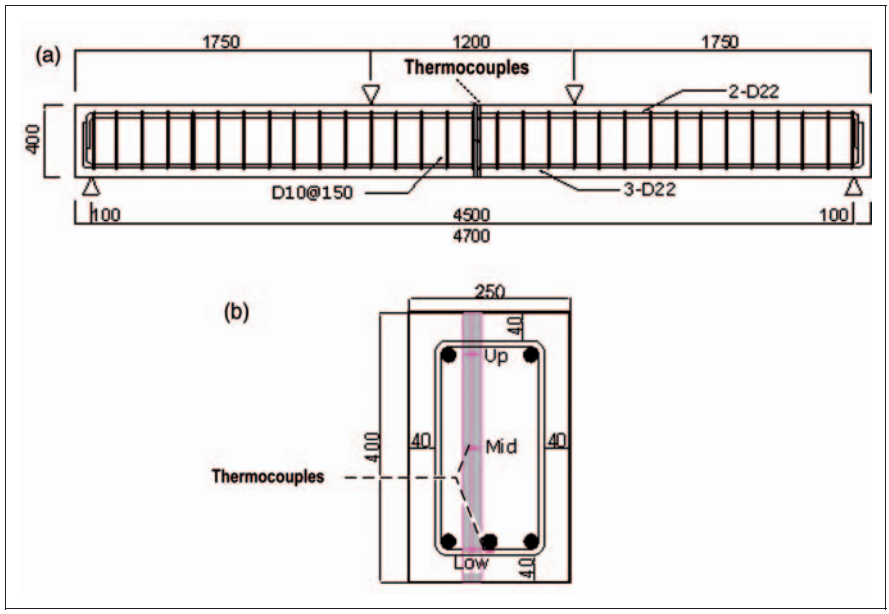

Figure 1. Configuration of beam specimens (mm): (a) dimensions of test specimen; (b) details of beam section (cover thickness = 40 mm).

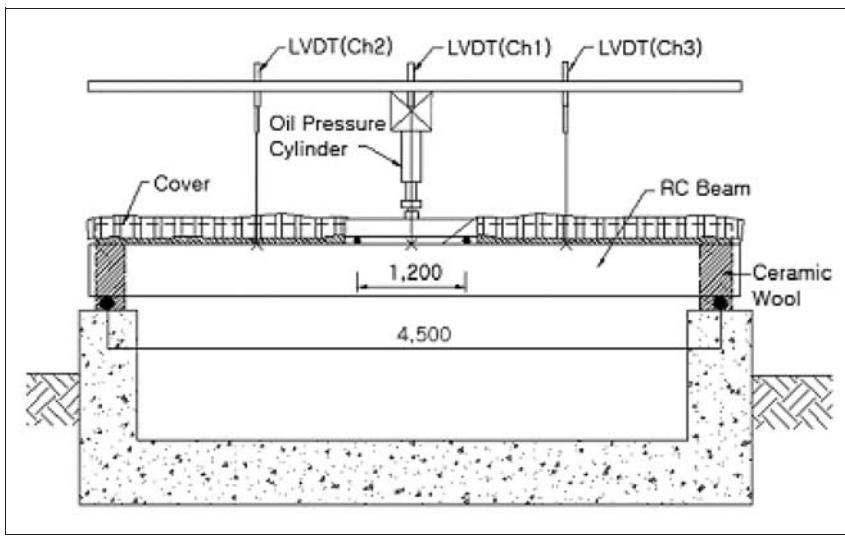

Figure 2. Test setup of a beam in heating furnace (mm).

ISO 834 standard time–temperature curve (Figure 3), and temperatures throughout the heating furnace are monitored from nine thermocouples. The average of temperatures measured from these thermocouples is used as the representative temperature of the heating furnace. In addition, linear variables displacement transducers (LVDTs) are placed at the center and 1/4 of the beam length to measure vertical displacements of the beams during the furnace heating.

Loading test

Four-point loading tests are performed to examine the structural behavior of the damaged RC beams 1 month after the furnace heating. The test setup is shown in Figure 4. The beams are simply supported with an effective length of 4000 mm.

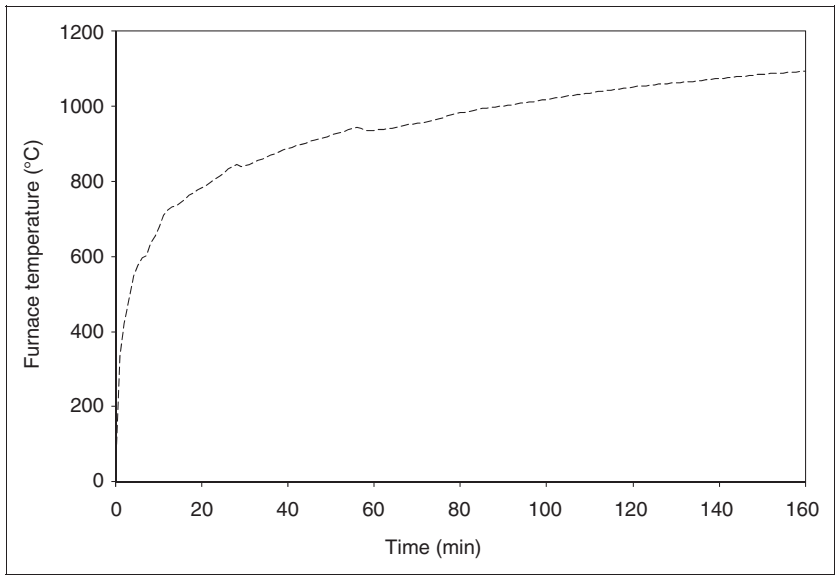

Figure 3. ISO 834 standard time–temperature curve.

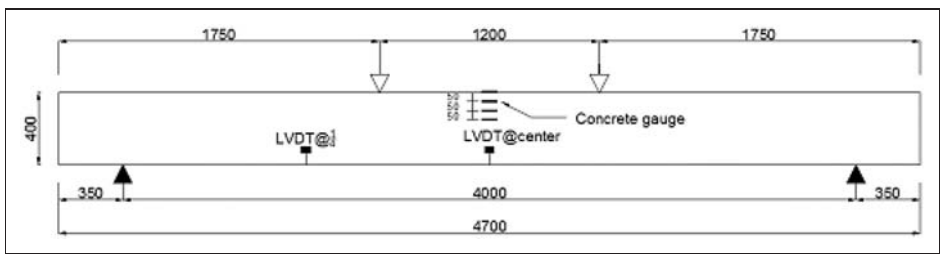

Figure 4. Four-point loading test setup (mm).

The load is applied through a load cell in a form of displacement control and LVDTs measure deflections during loading in the middle and 1/4 of the beam length. Three gages are attached on the upper side surface in the middle of the beam at 50 mm intervals to obtain compressive strains of concrete during loading.

Results

Thermal behavior of RC beams

Figure 5(a) and (b) shows the effect of cover thickness on the temperature distribution within RC beams having NSC. In comparing different cover thicknesses, maximum temperature is measured at the 'Low' location of the NSC beam with cover thickness of 40 mm, which shows about a 10% higher temperature in °C than the NSC beams with cover thickness of 50 mm. Also, temperatures of the longitudinal steel bars are much higher in the beam with cover thickness of 40 mm than the steel bars in the beams with cover thickness of 50 mm due to the former being closer to the heat source.

Figure 6(a) and (b) shows the effect of cover thickness on the temperature distribution within HSC beams. In HSC beams, the effect of cover thickness on the temperature distributions at 'Low' location is not as significant as in NSC, because the large amount of cover falls off due to spalling between 20 and 40 min of heating. However, in the 'Mid' location, a higher temperature is obtained in the HSC beam with cover thickness of 50 mm than the HSC beam with cover thickness of 40 mm, e.g. the maximum temperature at 'Mid' location is about 250°C for the beam with cover thickness of 50 mm, while it is 200°C for the beam with cover thickness of 40 mm. Also, the temperatures measured at 'Low' location are around 350°C when the HSC beams are heated for 90 min, while the NSC beams show 250°C at the same locations. The reason for showing the higher temperatures in HSC beams is

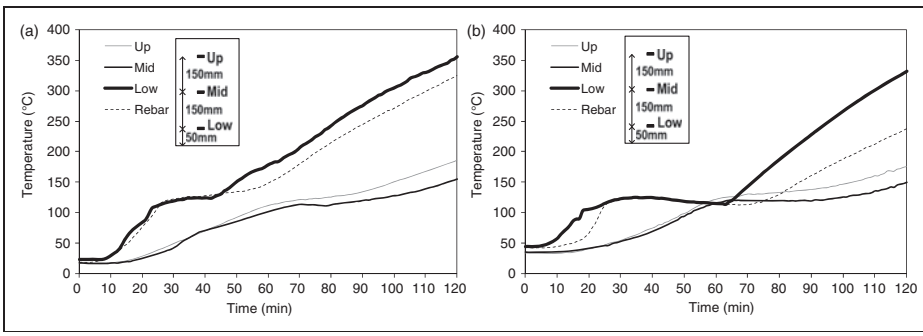

Figure 5. Temperature distributions of NSC beams: (a) NSC beams with cover thickness of 40 mm; (b) NSC beams with cover thickness of 50 mm.
NSC: normal-strength concrete.

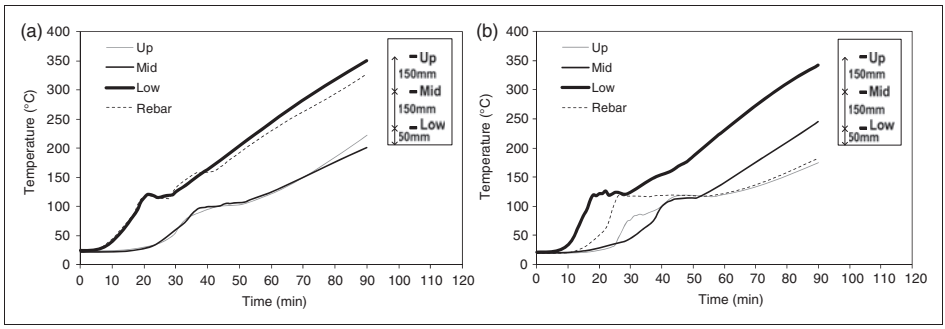

Figure 6. Temperature distributions of high-strength concrete beams: (a) HSC beams with cover thickness of 40 mm; (b) HSC beams with cover thickness of 50 mm.
HSC: high-strength concrete.

due to the spalling effect. When HSC beams are exposed to high temperatures, the concrete cover falls off due to spalling. Spalling in HSC beams under high temperatures is a well-known phenomenon and significantly related to structural behavior. Mostly, spalling in HSC beams occurs as pore pressure increases and tensile strength of concrete decreases [10]. In order to quantify spalling of HSC beams, cross sections of the beams after 90 min of furnace heating are measured at the locations along the beam length illustrated in Figure 7(a) and (b), indicating that the average area loss of the HSC beam with cover thickness of 50 mm is slightly larger than the HSC beam with cover thickness of 40 mm. When the beam has cover thickness of 40 mm, the remaining area after the cover thickness fell off due to spalling is about 82.7% of the original cross-sectional area, according to measurements observed from Figure 7(a). On the other hand, for the beam with cover thickness of 50 mm, the remaining area after the cover thickness fell off due to spalling is about 80.3% of the original cross-sectional area. Since a larger area remains in the beam with cover thickness of 40 mm, thermal conduction preceded more slowly, leading to lower temperatures in the interior portion of the beam compared to the beam with cover thickness of 50 mm, as observed from Figure 6(a) and (b). In fact, the effect of confinement on the temperature distributions or spalling also can be found from test results where variables are tie configurations or confinement. According to Kodur and Phan [9], HSC columns having provision of bent ties at 135° back into the core of the column and increased lateral reinforcement show improved fire endurance. These results confirm that a lower temperature distribution and a reduced amount of spalling can be achieved in beams with more confinement.

Structural behavior of damaged beams

Surface cracks of NSC beams caused by high temperatures are illustrated in Figure 8(a) and (b). In the NSC beams, the cover partly falls off, but spalling is not found.

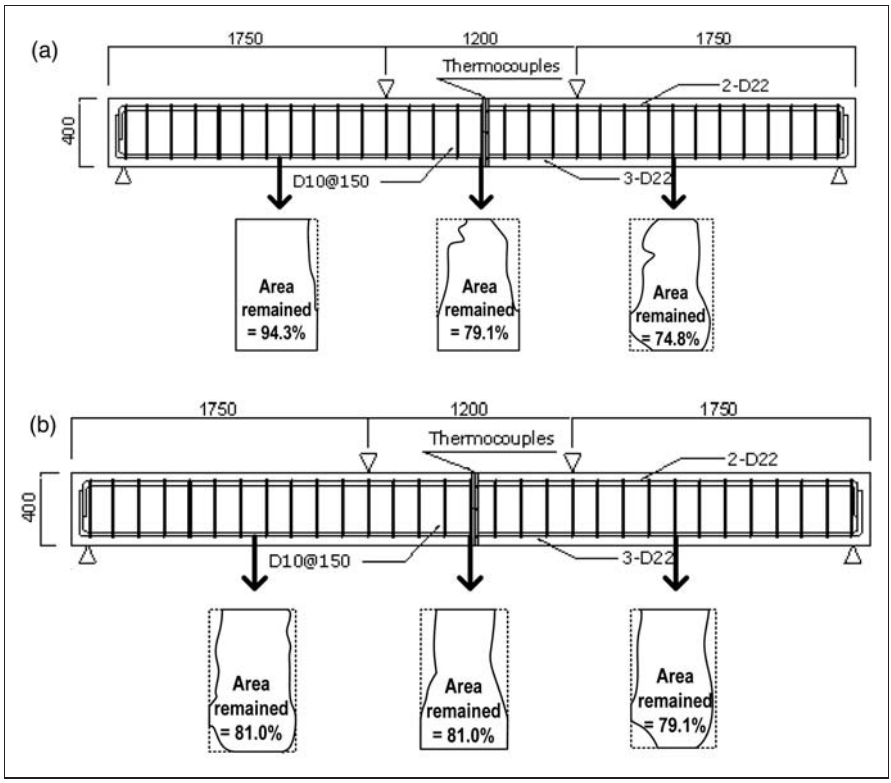

Figure 7. Cross sections of HSC beam measured at 1/4, center, and 3/4 of beam length: (a) HSC beams with cover thickness of 40 mm; (b) HSC beams with cover thickness of 50 mm. HSC: high-strength concrete.

As expected, more cracks occur as heating time increases from 60 to 120 min. The observed cracks are shallow and exist only on the surface. Between the NSC beams with cover thickness of 40 and 50 mm, slightly more cracks are observed from the beams with cover thickness of 50 mm. This can be explained from the lower load capacity of the NSC beams with cover thickness of 50 mm than the NSC beam with cover thickness of 40 mm. The NSC beams with cover thickness of 50 mm have effective depth of 350 mm, while the NSC beams with cover thickness of 40 mm have effective depth of 360 mm. Due to spalling, cracks of HSC beam surfaces are not observable.

During the loading tests performed 1 month after the furnace heating, flexural cracks due to loading are initiated from the cracks caused by high temperatures, especially from the middle of beam length, and propagate towards the upper and end of the beam, as illustrated in Figure 9(a) and (b). Comparing Figure 9(a)

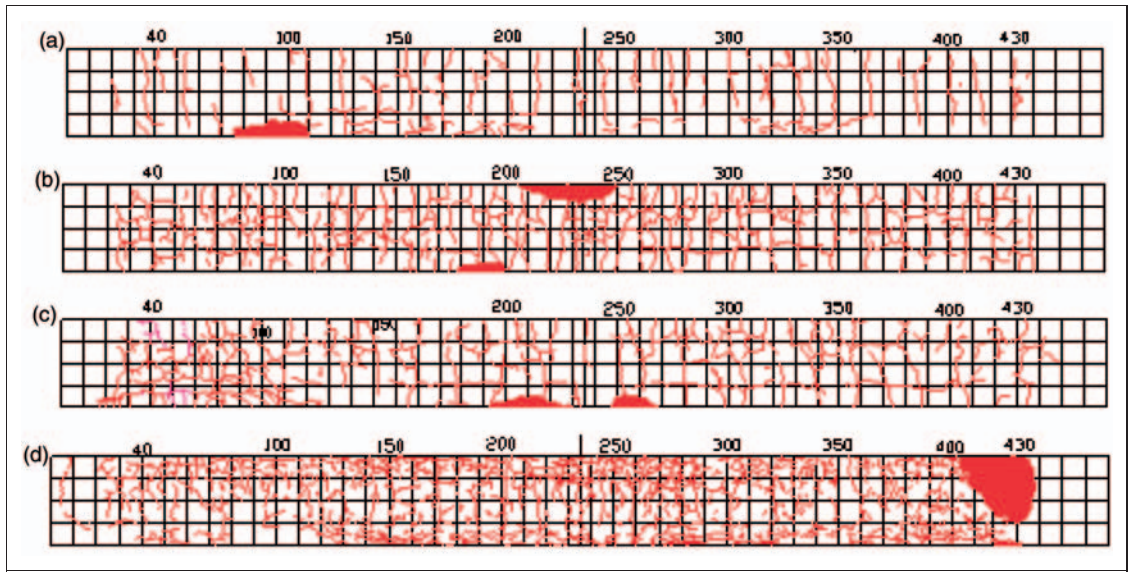

Figure 8. Cracks on the faces of NSC specimens after furnace heating: (a) NSC beams with cover thickness of 40 mm after 60 min of heating; (b) NSC beams with cover thickness of 40 mm after 120 min of heating; (c) NSC beams with cover thickness of 50 mm after 60 min of heating; and (d) NSC beams with cover thickness of 50 mm after 120 min of heating.
NSC: normal-strength concrete.

with (b), cracks of fire damaged NSC beams with cover thickness of 50 mm are distributed in a dispersed manner, while most of the cracks on the beams with cover thickness of 40 mm are seen in the middle area of the beam length. Also, load–deflection curves are obtained from the loading tests, as shown in Figure 10(a)

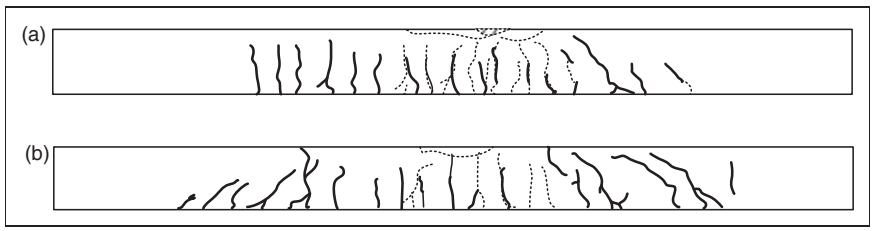

Figure 9. Cracks on the faces of NSC specimens after loading tests; thick lines are cracks due to loading and the dotted lines are large cracks due to high temperatures: (a) damaged NSC beams with cover thickness of 40 mm after loading tests; (b) damaged NSC beams with cover thickness of 50 mm after loading tests.
NSC: normal-strength concrete.

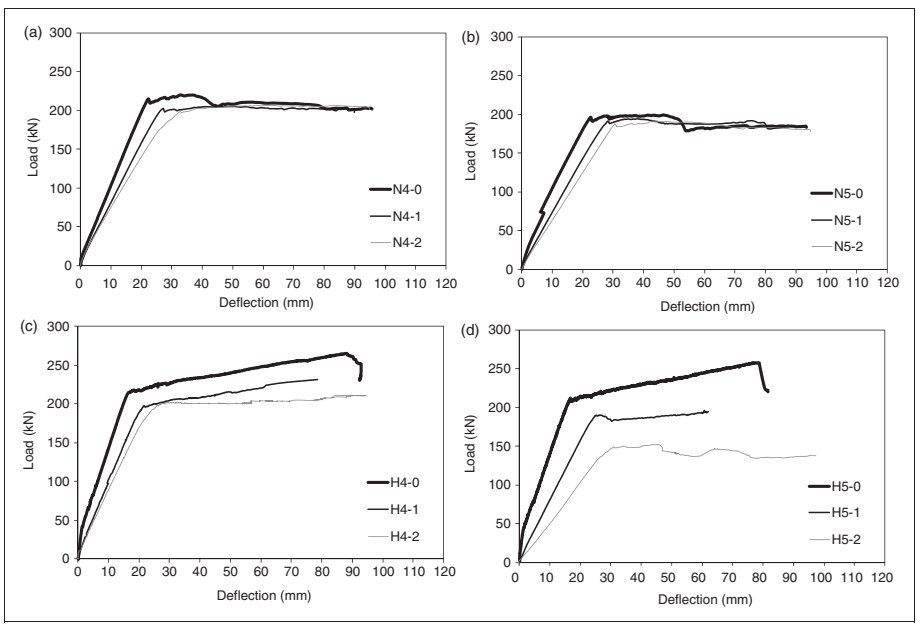

Figure 10. Load–deflection curves of the damaged RC beams: (a) NSC beams with cover thickness of 40 mm; (b) NSC beams with cover thickness of 50 mm; (c) HSC beams with cover thickness of 40 mm; and (d) HSC beams with cover thickness of 50 mm.
RC: reinforced concrete; NSC: normal-strength concrete; HSC: high-strength concrete.

Table 3. Ratio of maximum load of damaged RC beams to that of the undamaged beams.

Specimen	Maximum load (kN)	Ratio (%)	Specimen	Maximum load (kN)	Ratio (%)
N4-0	220.40	100	H4-0	265.05	100
N4-1	205.35	93	H4-1	231.75	87
N4-2	206.55	94	H4-2	227.10	86
N5-0	199.80	100	H5-0	257.40	100
N5-1	194.40	97	H5-1	202.05	79
N5-2	191.40	96	H5-2	139.20	54

RC: reinforced concrete.

through (d). In all tested beams, slopes of the load–deflection curves and the maximum loads decrease as the heating time increases. Especially, damaged HSC beams result in more degradation of structural performance as heating time increases compared with the damaged NSC beams. From the load–deflection curves of the damaged NSC beams, maximum loads are observed at the end of the elastic region of the load–deflection curves followed by long plateau until failure, while load–deflection curves of HSC beams are appeared as bi-linear and maximum loads are observed at the end of the plastic region with large deflections. When comparing maximum loads of the beams having different cover thicknesses, direct comparisons are not proper because effective depths are different for the beams having different cover thicknesses so that the load capacities are not same. For the case of NSC beams, nominal moments of the beams with cover thickness of 40 and 50 mm are 140.1 and 136.3 kN m, respectively. In order to compare structural behavior of the beams with different cover thicknesses, ratios of maximum loads of the damaged beams to the maximum loads of the undamaged beams are calculated as presented in Table 3. From Table 3, it is shown that maximum loads of NSC beams with cover thickness of 40 mm are 93–94% of that of the undamaged beams, while maximum loads of beams with cover thickness of 50 mm are 96–97% of that of the undamaged beams. So, the NSC beams with cover thickness of 50 mm show less structural damage than the NSC beams with cover thickness of 40 mm, mainly because the temperatures of the N5 series are slightly lower than the temperatures of N4 series due to the larger cover thickness. However, differences of load ratios between the NSC beams with cover thickness of 40 and 50 mm are very small, as their temperature differences are not significant. In addition, the difference of the reduced maximum loads between 60 and 120 min of heating time is not significant in the NSC beams.

As for the HSC beams, load–deflection curves appeared as bi-linear and maximum loads are observed at the end of the plastic region with large deflections. Also, maximum loads of the damaged HSC beams decrease about 13–46% depending on heating time and cover thickness, as presented in Table 3. The larger reduction of the maximum load is observed from the HSC beams rather than the NSC

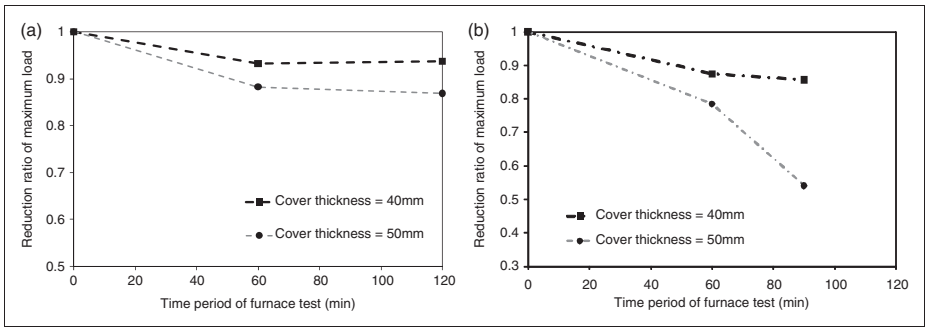

Figure 11. Maximum load reduction ratio: (a) NSC beams and (b) HSC beams.
NSC: normal-strength concrete; HSC: high-strength concrete.

beams, because spalling of the damaged HSC beams results in reduction of second moment of area. Since the cover falls out due to spalling, the HSC beams with cover thickness of 50 mm result in more damage than the HSC beams with cover thickness of 40 mm. Also, the maximum loads of the HSC beams, especially for the beams with cover thickness of 50 mm, decreases a large amount as the heating time increases.

From the loading test results, relationships between reduction ratio of maximum load and heating time are found, as illustrated in Figure 11(a) and (b). Overall, the load capacity of the damaged RC beams decreases rapidly until 60 min of heating, and stabilizes towards the end of the furnace heating. It is interesting to note that the rate of load-capacity reduction increases with the heating time in the HSC beams with cover thickness of 50 mm. In this case, a large amount of spalling occurred during the furnace heating, which results in loss of cross-sectional area and degradation of loading capacity. Also, the stiffness of the damaged RC beams is defined from the slope of the load–deflection curves, and expressed as a function of heating time in Figure 12(a) and (b). Compared with the reduction ratio of maximum load, the stiffness decreases with the larger ratios, but similar tendencies are observed between cover thickness of 40 and 50 mm. From Figure 12(a) and (b), it is shown that stiffness reduction rate of NSC beams stabilizes as heating time increases, while the stiffness of HSC beams decreases continuously as heating time increases.

Discussion

From these experimental findings, a regression analysis is performed to propose an equation that can predict the reduction ratio of maximum load capacity and stiffness of the damaged RC beams. The proposed equation is in an exponential form as shown in equation (1). In this equation, R represents either the reduction ratio of maximum load capacity or the stiffness and therefore is dimensionless. Also, t is

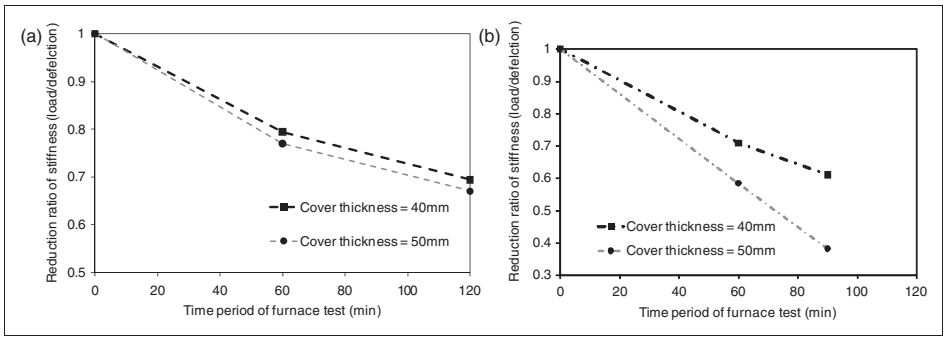

Figure 12. Stiffness reduction ratio: (a) stiffness reduction of NSC beams and (b) stiffness reduction of HSC beams.
NSC: normal-strength concrete; HSC: high-strength concrete.

Table 4. Values of *A* for the proposed equation.

		Cover thickness = 40 mm	Cover thickness = 50 mm
NSC	Maximum load capacity reduction ratio	−0.0007	−0.0004
	Stiffness reduction ratio	−0.0032	−0.0042
HSC	Maximum load capacity reduction ratio	−0.0019	−0.0060
	Stiffness reduction ratio	−0.0055	−0.01015

NSC: normal-strength concrete; HSC: high-strength concrete.

heating time in minutes (or time period of heating in minutes) and A is a constant. Units for t and A are min and 1/min, respectively. Values for A are varied depending on the concrete compressive strength and cover thickness as listed in Table 4.

$$R = \exp^{At} \tag{1}$$

Figure 13(a) through (d) illustrates reduction ratios predicted from the proposed equation compared with the experimental results. As shown in Figure 13(a) through (d), predicted results are in good agreement with the experimental results and the overall error between the prediction and the experimental results is about 1.4–11.1%. However, the predictions are found to be non-conservative for the case of NSC beams at 60 min and HSC beams at 90 min of heating. Using the limited number of variables and experimental results available, the coefficient A is determined so as to have the least error compared with experimental results. This coefficient needs to be refined as more results from sensitivity tests are accumulated from further studies.

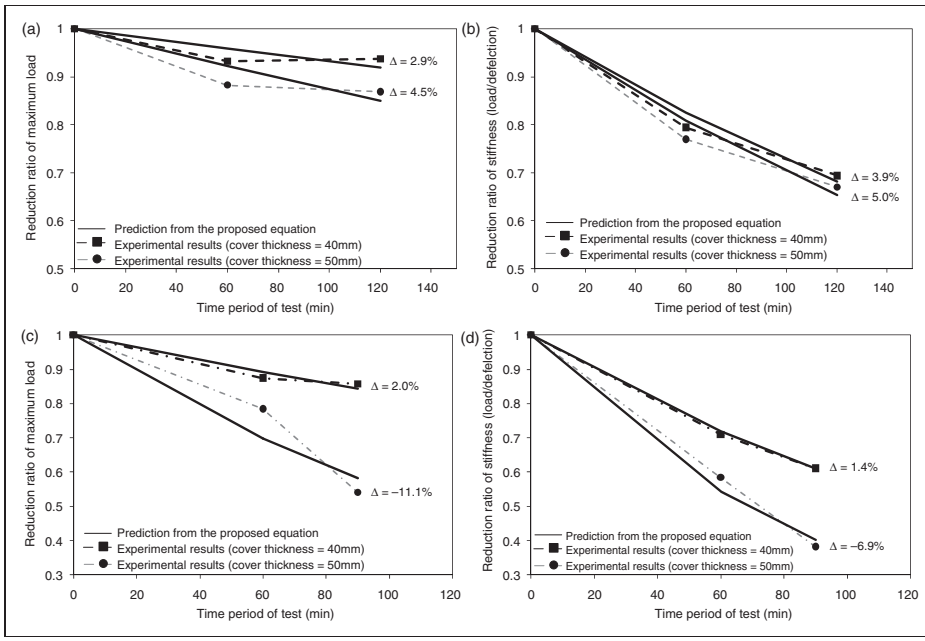

Figure 13. Predictions from the proposed equations compared with the experimental results: (a) maximum load reduction of NSC beams; (b) stiffness reduction of NSC beams; (c) maximum load reduction of HSC beams; and (d) stiffness reduction of HSC beams.
HSC: high-strength concrete; NSC: normal-strength concrete.

Conclusions

This study reports the effect of concrete strength and cover thickness on the thermal and structural behavior of RC beams under high temperatures. Normal and high-strength concrete beams are prepared to have 40 or 50 mm of cover thickness and exposed to high temperatures for time periods of 60, 90, or 120 min. Temperature distributions, spalling, and crack configurations of the RC beams during furnace heating are examined. From four-point loading tests performed on the damaged RC beams, maximum load capacity, stiffness, and crack propagation of the damaged beams are investigated. In addition, an equation for predicting reduction ratios of maximum load and stiffness of damaged RC beam is proposed as an exponential function. Based on this study, the following conclusions can be drawn:

1. Temperatures are much higher in HSC beams than the NSC beams because of spalling.
2. In NSC beams, the larger cover thickness results in the lower temperatures. However, in HSC beams, there is no difference of temperatures at 'Low' location

between the cover thickness of 40 and 50 mm and temperatures at 'Mid' location are higher in 50 mm cover thickness because of spalling.
3. From the loading tests of the damaged RC beams, HSC beams show more structural damage than the NSC beams due to spalling.
4. Comparing beams with cover thickness of 40 and 50 mm, the larger reductions of maximum load capacity and stiffness are observed from the beams with cover thickness of 50 mm.
5. The experimental results show that the rate of load capacity and stiffness reduction ratio changes with heating time, and can be expressed as an exponential function of heating time. With a proper value of the constant A, the proposed equation shows good agreement with the experimental results. However, the results from the proposed equation are compared to a limited number of experimental results such as normal and high-strength concrete beams with cover thicknesses of 40 and 50 mm subjected to the ISO 834 heating curve. Further studies are needed to see if the proposed equation is applicable to RC beams of different size, concrete strength, reinforcing ratio, and heating environment. Also, the coefficient A can be defined as a function of these same influencing parameters, such as beam size, concrete strength, cover thickness, reinforcing ratio, and heating environment.

Funding

This study was supported by grant no. R01-2008-000-20527-0 from the Basic Research Program of the Korea Science & Engineering Foundation.

References

1. Harmathy TZ. *Properties of building materials at elevated temperatures*. DRP Paper No. 1080 of the Division of Building Research, 1983. Ottawa: National Research Council of Canada.
2. Harmathy TZ. Properties of building materials. In: DiNenno PJ, et al. (eds) *SFPE handbook of fire protection engineering*. Bethesda, MD: Society of Fire Protection Engineers and National Fire Protection Association, 1988, pp.378–391.
3. ACI Committee 216. *Guide for determining the fire endurance of concrete elements*. American Concrete Institute Committee Report, 216R1-48, 1994, Farmington Hills, MI: ACI Committee.
4. ENV. Eurocode 2: design of concrete structures – part 1–2: general rules – structural fire design, 1992-1-2. European Committee for Standardization, 1995.
5. Kodur VKR and Sultan MA. The effect of temperature on thermal properties of high-strength concrete. *ASCE J Mater Civil Eng* 2003; 15(2): 101–107.
6. Cheng FP, Kodur VKR and Wang TC. Stress-strain curves for high strength concrete at elevated temperatures. *J Mater Civil Eng ASCE* 2004; 16(1): 84–90.
7. Kodur VKR, Cheng FP, Wang TC, et al.. Effect of strength and fiber reinforcement on fire resistance of high-strength concrete columns. *ASCE J Struct Eng* 2003; 129(2): 253–259.

8. Kodur VKR and McGrath R. Fire endurance of high strength concrete columns. *Fire Technol* 2003; 39: 73–87.
9. Kodur VKR and Phan LT. Critical factors governing the fire performance of high strength concrete systems. *Fire Saf J* 2007; 42: 482–488.
10. Dwaikat MB and Kodur VKR. Fire induced spalling in high strength concrete beams. *Fire Technol* 2010; 46: 251–274.
11. Kalifa P, Menneteau FD and Quenard D. Spalling and pore pressure in HPC at high temperatures. *Cem Concr Res* 2000; 30: 1915–1927.
12. Lee SJ. *Strength evaluation of fire-damaged normal strength concrete*. MS Thesis, Ewha Womans University, Seoul, South Korea, 2003.
13. Shin MK. *Strength evaluation of fire-damaged high strength concrete*. MS Thesis, Ewha Womans University, Seoul, South Korea, 2004.
14. Kim HS. *Strength evaluation of fire damaged high strength concrete by nondestructive tests*. MS Thesis, Ewha Womans University, Seoul, South Korea, 2004.
15. Choi EG. *Performance assessment of high strength concrete members subjected to fire*. PhD Thesis, Ewha Womans University, Seoul, South Korea, 2008.
16. Haj-Ali RM, Choi J and Kim HS. Integrated fire dynamics and thermomechanical modeling framework for steel-concrete composite structures. *Steel Compos Struct Int J* 2010; 10(2): 129–149.
17. Choi J, Haj-Ali RM and Kim HS. Integrated fire dynamic and thermomechanical modeling of a bridge under fire. *Struct Eng Mech* 2012; 42(6): 815–829.